perimental values for the perpendicular haloalkene triplets since only minimum ISC rates could be obtained; however, the prediction as well is clearly for lifetimes shorter than our observation limit.

These results show that heavy atom effects of chlorine can be far larger than previously reported and highlight the role of nonplanar geometries in the enhancement of SOC even for heavy atoms. The range of possible analogous effects on biradicals and the magnitude of effects due to other third-row elements are under study.

Acknowledgment. We thank the National Science Foundation for financial support (Grants 8516534 and 8820268). Flash kinetics were performed at The Center for Fast Kinetics Research at The University of Texas at Austin, supported by NIH Grant RR-00886.

Registry No. $(Ph)_2C{=}CH_2$, 530-48-3; $(Ph)_2C{=}C(Cl)_2$, 2779-69-3; $(Ph)_2C{=}CHCH_3$, 778-66-5; $(Ph)_2C{=}C(Cl)CH_3$, 781-34-0; $(Ph)_2C{=}C(CH_3)_2$, 781-33-9; $ClCH{=}CH_2$, 75-01-4; 1*H*-indene, 95-13-6; 2-chloro-1*H*-indene, 18427-72-0; 1,2-dihydronaphthalene, 447-53-0; 3-chloro-1,2-dihydronaphthalene, 138384-40-4.

The Photochemistry of Transition Metal Hydrides: A CASSCF/CCI Study of the Photodissociation of $HMn(CO)_5$

Chantal Daniel

Contribution from the Laboratoire de Chimie Quantique, U.P.R. 139 du CNRS, Institut Le Bel, F-67000 Strasbourg, France. *Received June 27, 1991*

Abstract: The photodissociation of $HMn(CO)_5$ has been studied through contracted configuration interaction calculations of the potential energy surfaces for the metal–hydrogen bond homolysis and the dissociation of the carbonyl ligand. The corresponding potential energy curves connect the ground and excited states of the reactant to the ground and excited states of the primary products. The calculations were carried out under C_{4v} constraint with a basis set that is at least of double-ζ quality. The multireference CCI calculations that correlate the 3d electrons and the two of the Mn–H bond were based on a unique CASSCF wave function with eight electrons in nine active orbitals ($3d_{xy}$, $3d_{\pi}$, σ_{Mn-H}, σ^*_{Mn-H}, $3d_{x^2-y^2}$, $4d_{xy}$, $4d_{\pi}$) optimized for the $^5A_2$ state, the principal cnfiguration being $(3d_{xy})^2(3d_{\pi})^2(\sigma)^2(\sigma^*)^1(3d_{x^2-y^2})^1$. It is proposed that excitation of $HMn(CO)_5$ at 193 nm will bring the molecule from the ground state a^1A_1 into the c^1E d $\rightarrow \pi^*$ excited state. From there, after intersystem crossing to the b^3A_1 at a Mn–H distance of about 1.7 Å and internal conversion into the a^3A_1 $\sigma \rightarrow \sigma^*$ state, the molecule will dissociate along the a^3A_1 potential energy curve to the products H and $Mn(CO)_5$ in their ground state. Irradiation of $HMn(CO)_5$ at 229 nm will bring the molecule into the b^1E state $d_{\pi} \rightarrow \sigma^*$. Then the system goes down along the b^1E potential energy curve corresponding to the Mn–CO elongation until it reaches a potential well. From there after internal conversion to the a^1E state the molecule will dissociate along the corresponding potential energy curve to the products CO and $HMn(CO)_4$ in the a^1E excited state with the fragment $HMn(CO)_4$ as a square pyramid with H apical. The main reasons responsible for the different behavior, upon irradiation, of the two hydrides $HCo(CO)_4$ and $HMn(CO)_5$ are outlined on the basis of these results.

Introduction

The photoreactivity of transition metal hydrides was mainly used to generate very active intermediates with a role in many catalytic processes and chemical reactions.[1] Monohydride complexes were shown to undergo a variety of photochemical reactions with experimental evidence obtained for both the homolysis of the metal–hydrogen bond[2-4] and the photoinduced ligand dissociation,[5-10] the latter being the dominant process. In spite of the intense experimental activity developed in this field during the last decade, mainly due to the improvement of new identification techniques, the mechanism of the primary photochemical reaction is partially understood and the nature of the photoactive excited states responsible for the photodissociation pathways is uncertained.

The first theoretical analysis of the photochemical reactions for organometallics[11] was based on molecular orbital diagrams. More recently, the use of state correlation diagrams,[12-16] potential energy surfaces (PES), or the more readily visualized potential energy curves (PEC)[17-23] has enabled us to get a better under-

(1) Geoffroy, G. L. *Prog. Inorg. Chem.* **1980**, *27*, 123.
(2) Hoffman, N. W.; Brown, T. L. *Inorg. Chem.* **1978**, *17*, 613.
(3) Endicott, J. F.; Wong, C. L.; Inoue, T.; Natarajan, P. *Inorg. Chem.* **1979**, *18*, 450.
(4) Grebenik, P.; Downs, A. J.; Greens, M. L. H.; Perutz, R. N. *J. Chem. Soc., Chem. Commun.* **1979**, 742.
(5) Rest, A. J.; Turner, J. J. *J. Chem. Soc., Chem. Commun.* **1969**, 375.
(6) Mills, W. J.; Clark, R. J. *Inorg. Chem.* **1968**, *7*, 1801.
(7) Beyers, B. H.; Brown, T. L. *J. Am. Chem. Soc.* **1977**, *99*, 2527.
(8) Werner, P.; Ault, B. S.; Orchin, M. *J. Organomet. Chem.* **1978**, *162*, 189.
(9) Conder, H. L.; Courtney, A. R.; DeMarco, D. *J. Am. Chem. Soc.* **1979**, *101*, 1606.
(10) Geoffroy, G. L.; Bradley, M. G. *Inorg. Chem.* **1977**, *16*, 744.
(11) Geoffroy, G. L.; Wrighton, M. S. *Organometallic Photochemistry*; Academic Press: New York, 1979.
(12) Veillard, A. *New J. Chem.* **1981**, *5*, 599.
(13) Veillard, A.; Dedieu, A. *New J. Chem.* **1983**, *7*, 683.
(14) Veillard, A.; Dedieu, A. *Theor. Chim. Act.* **1983**, *63*, 339.
(15) Daniel, C.; Veillard, A. *New J. Chem.* **1986**, *10*, 83.
(16) Rohmer, M. M. *Chem. Phys. Lett.* **1989**, *157*, 207.
(17) Daniel, C.; Bénard, M.; Dedieu, A.; Wiest, R.; Veillard, A. *J. Phys. Chem.* **1984**, *88*, 4805.
(18) Daniel, C.; Hyla- Kryspin, I.; Demuynck, J.; Veillard, A. *Nouv. J. Chim.* **1985**, *9*, 581.
(19) Veillard, A.; Daniel, C.; Strich, A. *Pure Appl. Chem.* **1988**, *60*(2), 215.
(20) Veillard, A.; Strich, A. *J. Am. Chem. Soc.* **1988**, *110*, 3793.
(21) Daniel, C. *Coordination Chemistry Reviews*, Proceedings of the 8th International Symposium on the Photochemistry and Photophysics of Coordination Compounds, 1990; Elsevier Science Publishers B. V.: Amsterdam; Vol. 97, p 141.
(22) Daniel, C. *J. Phys. Chem.* **1991**, *95*, 2394.
(23) Rohmer, M. M.; Veillard, A. *New J. Chem.* **1991**, *15*, 795.

0002-7863/92/1514-1625$03.00/0

standing of the mechanism of different types of photochemical reactions: (i) the heterolytic loss of a carbonyl ligand; (ii) the homolysis of a metal–hydrogen, metal–metal, or metal–alkyl bond; (iii) the photoelimination of molecular hydrogen; and (iv) the photosubstitution reactions in d^6 carbonyl complexes. From our last theoretical studies of transition metal hydrides,[24,25] we have deduced that if the ligand field states corresponding to $d \rightarrow d$, $d \rightarrow \sigma^*$ excitations are probably responsible for the ligand dissociation, the homolysis of the metal–hydrogen bond results from the dissociative character of the triplet-state potential energy curve corresponding to the $\sigma_{M-H} \rightarrow \sigma^*_{M-H}$ excitation.

One exciting aspect of the photochemistry of organometallics is the occurrence upon irradiation of two photochemical processes, either at a unique wavelength or at different wavelengths. Typical examples include the hydrides $HCo(CO)_4$[26,27] and $HMn(CO)_5$:[5,28,30]

$$HCo(CO)_4 \xrightarrow{h\nu} H + Co(CO)_4 \quad \text{minor} \qquad (1)$$

$$HCo(CO)_4 \xrightarrow{h\nu} CO + HCo(CO)_3 \quad \text{major} \qquad (2)$$

$$HMn(CO)_5 \xrightarrow{h\nu} H + Mn(CO)_5 \quad \text{minor} \qquad (3)$$

$$HMn(CO)_5 \xrightarrow{h\nu} CO + HMn(CO)_4 \quad \text{major} \qquad (4)$$

More recently, qualitative solution photochemistry studies have shown that both CO loss and Mn–R homolysis do occur in $RMn(CO)_5$[3,31-41] (R = CH_3, CH_2SiMe_3, $CH_2C_6H_5$, η^1-$C_6H_5CH_2$, C_6H_5, C_6F_5, C_2F_4H, η^1-C_5Cl_5).

$$RMn(CO)_5 \xrightarrow{h\nu} RMn(CO)_4 + CO \qquad (5)$$

$$RMn(CO)_5 \xrightarrow{h\nu} R + Mn(CO)_5 \qquad (6)$$

In connection with the loss of a carbonyl ligand (eq 5), Young and Wrighton[41] reported the possibilities of equatorial and axial labilization following photoexcitation of $RMn(CO)_5$ (R = η^1-C_5Cl_5, η^1-$C_6H_5CH_2$) with a higher excitation energy favoring equatorial CO loss. Moreover, an interesting theoretical question still remains to be answered, namely, why $RMn(CO)_4$ (R = H, CH_3) as a square pyramid with R basal seems to be the predominant isomer identified in low-temperature matrixes experiments.[28,42]

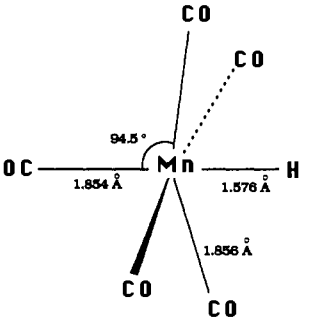

Figure 1. Structure of $HMn(CO)_5$.[44]

Scheme I

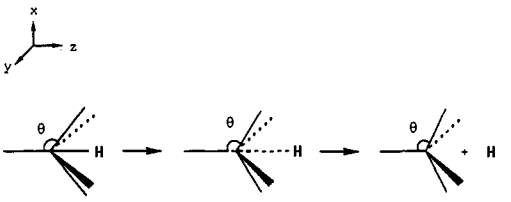

Scheme II

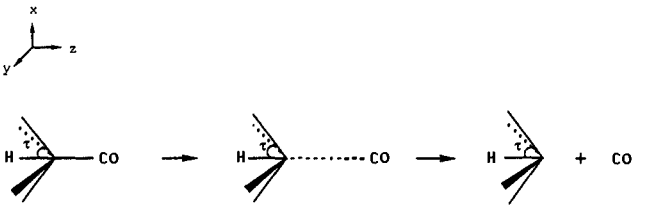

In order to explain the mechanism of photodissociation and the existence of two concurrent dissociative channels in $HCo(CO)_4$, we have investigated the excited states and the corresponding PES of this system.[18-20] On the basis of these results and of the calculated excited states of $HMn(CO)_5$,[43] we have tried to compare the photochemistry of $HCo(CO)_4$ and $HMn(CO)_5$. According to experimental data,[5,26-30] the dissociation of the carbonyl ligand is the dominant process in both cases, hydrogen and carbonyl loss occurring at the same wavelength (254 nm) for $HCo(CO)_4$. On the other hand, low-temperature matrix experiments reported for $HMn(CO)_5$[28-30] indicate an extremely low quantum yield for reaction 3. The formation of $Mn(CO)_5$ upon irradiation by conventional UV photolysis (229 nm) is not well established and does occur under particular conditions. Evidence for reaction 3 comes from irradiation of $HMn(CO)_5$ at 193 nm.[28] In the absence of PES for $HMn(CO)_5$ it has been difficult to rationalize the photochemical behavior of this system.

With the intention of comparing the photoreactivity of these two transition metal hydrides and since $HMn(CO)_5$ represents an excellent model for a preliminary study of the photochemical behavior of the $RMn(CO)_5$ systems, we decided to investigate in a more refined treatment the photodissociation of $HMn(CO)_5$. The aim of the present study is the calculation of the potential energy surfaces for the two photochemical processes of $HMn(CO)_5$ corresponding to the homolysis of the Mn–H bond and to the dissociation of a carbonyl ligand, through contracted configuration interaction (CCI) calculations based on complete active space self-consistent field (CASSCF) reference wave functions.

Computational Details

The calculations for $HMn(CO)_5$ were performed for the experimental geometry[44] that is of C_{4v} symmetry (Figure 1). It has been assumed that the C_{4v} symmetry is retained along the reaction path corresponding to the homolysis of the metal–hydrogen bond (Scheme I), since $Mn(CO)_5$

(24) Veillard, A. *Chem. Phys. Lett.* **1990**, *170*, 441.
(25) Daniel, C.; Veillard, A. *Theoretical Studies of the Photochemistry of Transition Metal Hydrides*. In *Transition Metal Hydrides*; Dedieu, A., Ed.; VCH Publishers, Inc.: New York, 1991; pp 235–261.
(26) Sweany, R. L. *Inorg. Chem.* **1980**, *19*, 3512.
(27) Sweany, R. L. *Inorg. Chem.* **1982**, *21*, 752.
(28) Church, S. P.; Poliakoff, M.; Timney, J. A.; Turner, J. J. *Inorg. Chem.* **1983**, *22*, 3259.
(29) Church, S. P.; Poliakoff, M.; Timney, J. A.; Turner, J. J. *J. Am. Chem. Soc.* **1981**, *103*, 7515.
(30) Symons, M. C. R.; Sweany, R. L. *Organometallics* **1982**, *1*, 834.
(31) Pourreau, D. B.; Geoffroy, G. L. *Adv. Organomet. Chem.* **1985**, *24*, 249.
(32) Hudson, A.; Lappert, M. F.; Lednor, P. W.; Nicholson, B. K. *J. Chem. Soc., Chem. Commun.* **1974**, 966.
(33) Bamford, C. H.; Mullik, S. U. *J. Chem. Soc., Faraday Trans.* **1979**, *1*, 2562.
(34) Lipps, W.; Kreiter, C. G. *J. Organomet. Chem.* **1983**, *241*, 185. Kreiter, C. G.; Lipps, W. *J. Organomet. Chem.* **1983**, *253*, 339.
(35) Ogilvie, J. F. *J. Chem. Soc., Chem. Commun.* **1970**, 323.
(36) McHugh, T. M.; Rest, A. J. *J. Chem. Soc., Dalton Trans.* **1980**, 2323.
(37) Hudson, A.; Lappert, M. F.; Lednor, P. W.; Macquitty, J. J.; Nicholson, B. K. *J. Chem. Soc., Dalton Trans.* **1981**, 2159.
(38) Gismondi, T. E.; Rausch, M. D. *J. Organomet. Chem.* **1985**, *284*, 59.
(39) Miles, J. R.; Clark, R. J. *Inorg. Chem.* **1968**, *7*, 1801.
(40) Olivier, A. J.; Graham, W. A. *Inorg. Chem.* **1970**, *9*, 2578.
(41) Young, K. M.; Wrighton, M. S. *J. Am. Chem. Soc.* **1990**, *112*, 157.
(42) Horton-Mastin, A.; Poliakoff, M.; Turner, J. J. *Organometallics* **1986**, *5*, 405.
(43) Veillard, A.; Strich, A.; Daniel, C.; Siegbahn, P. E. M. *Chem. Phys. Lett.* **1987**, *141*, 329.
(44) McNeill, E. A.; Scholer, F. R. *J. Am. Chem. Soc.* **1977**, *99*, 6243.

Table I. CASSCF and CCI Calculations

CASSCF

state	main configuration	active space
$^5A_2$	$(3d_{xy})^2(3d_\pi)^2(\sigma)^2(\sigma^*)^1(3d_{x^2-y^2})^1$	8e 9a

CCI

valence space	no. of electrons correlated	no. of reference states[a]	no. of config[a]
$3d_{xy}$, $3d_\pi$, $3d_{x^2-y^2}$, σ, σ^*	8	2 to 5	26 193 to 298 125

[a] The number of reference states and of configurations depend on the characteristics of the calculated state (symmetry, spin).

has C_{4v} symmetry in its ground state.[29,45]

For the sake of simplicity, the loss of an axial ligand which produces $HMn(CO)_4$ as a square pyramid of C_{4v} symmetry with the hydrogen atom in apical position has been considered for the photodissociation of a carbonyl ligand from $HMn(CO)_5$. For this reason we have assumed that the C_{4v} symmetry is retained along the reaction path (Scheme II). Those assumptions can be justified by the fact that the symmetry restrictions usually affect the energy profiles characterized by the presence of high-energy barriers.[46] The symmetry constraints should not operate dramatically on the smooth profile of the excited potential energy curves which are going to govern the mechanism of the photochemical reaction.

The bond lengths were kept constant and equal to the experimental values[44] (except for the bond which dissociates). For the dissociation of the metal–hydrogen bond (Scheme I) the angle θ was kept constant to 94.5°, that is the experimental value of this angle in the reactant $HMn(CO)_5$[44] (the optimized value at the SCF level[45] in the primary product $Mn(CO)_5$ being 95.8° versus an experimental estimation of 96°[29]). The angle τ (Scheme II) was kept constant to 85.5° along the reaction path corresponding to the dissociation of the carbonyl ligand (the experimental value of τ being 85.5° for $HMn(CO)_5$ versus an optimized value of 85° for $HMn(CO)_4$ at the SCF level[45]).

The following basis sets were used: for the manganese atom a (15, 11, 6) set contracted to [9, 6, 3],[47] for the first-row atoms a (10, 6) set contracted to [4, 2],[50] and for hydrogen a (6, 1) set contracted to [3, 1].[51] This basis set is triple-ζ for the 1s shell of hydrogen and for the 3d and 4s shells of the manganese atom; otherwise, it is double-ζ.

The CASSCF calculations[52] were carried out to obtain wave functions which are used as references for the CCI calculations.[53] The rigorous way to calculate potential energy surfaces consists of carrying out for each electronic state a CASSCF calculation followed by a contracted CI calculation.[55] However, in spite of its accuracy this sophisticated method is not adapted to the studies reported here for two reasons: (i) this procedure is very expensive; (ii) the convergence of the CASSCF may be hazardous when we deal with problems characterized by many excited states in a same symmetry.[56] A detailed description of a more economical computational strategy to reproduce correctly the sequence and energetics of the electronic states of $HMn(CO)_5$ is described elsewhere.[43] Ab initio potential energy curves are obtained from CCI calculations based on a unique CASSCF reference wave function. Details of the CASSCF calculation are reported in Table I, in which the active space is described by the number of electrons correlated (ne) and the number of active orbitals (na).

Table II. Calculated CCI Excitation Energies (in cm^{-1}) for the Lowest States of $HMn(CO)_5$

	one-electron excitation in the principal configuration	
$a^1A_1 \rightarrow a^3E$	$3d_\pi \rightarrow 3d_{x^2-y^2}$	23 940
$a^1A_1 \rightarrow b^3E$	$3d_\pi \rightarrow \sigma^*$	32 940
$a^1A_1 \rightarrow {}^3A_2$	$3d_{xy} \rightarrow 3d_{x^2-y^2}$	33 020
$a^1A_1 \rightarrow a^1E$	$3d_\pi \rightarrow 3d_{x^2-y^2}$	33 580
$a^1A_1 \rightarrow a^3A_1$	$3d_{xy} \rightarrow 4d_{xy}$	38 230
$a^1A_1 \rightarrow {}^1A_2$	$3d_{xy} \rightarrow 3d_{x^2-y^2}$	38 500
$a^1A_1 \rightarrow b^1E$	$3d_\pi \rightarrow \sigma^*$	43 150
$a^1A_1 \rightarrow c^1E$	$3d_\pi \rightarrow \pi^*$	53 990
$a^1A_1 \rightarrow b^3A_1$	$\sigma \rightarrow \sigma^*$	61 670

Because we focus on the lowest excited states that are of $d \rightarrow d$, $d \rightarrow \sigma^*$, and $\sigma \rightarrow \sigma^*$ type, this CASSCF calculation was carried out for a selected[43] high-spin state $^5A_2$ in which the occupation number of the orbitals σ^* and d, vacant in the ground state, is 1 (σ and σ^* denote the molecular orbitals that are respectively, bonding and antibonding with respect to the metal–hydrogen bond). The principal configuration for this $^5A_2$ state is $(3d_{xy})^2(3d_\pi)^2(\sigma)^2(\sigma^*)^1(3d_{x^2-y^2})^1$. The CASSCF space was limited to nine molecular orbitals, corresponding to the 3d orbitals of the manganese (d_{xy}, d_π, $d_{x^2-y^2}$), the $4d_{xy}$ and $4d_\pi$ orbitals that correlate them, and the σ and σ^* orbitals. Eight electrons are correlated in these calculations.

For each electronic state, two CCI calculations were performed: the first with one reference corresponding to the required state, the second being a multireference calculation including all the configurations that appear with a coefficient larger than 0.08 in the monoreference CI wave function. In this work we report only the results of the multireference calculations. Details of the CCI calculations are given in Table I. Eight electrons are correlated in these calculations (the 3d electrons and those of the Mn–H bonds). Single and double excitations to all virtual orbtials, except the counterparts of the carbonyls 1s and of the metal 1s, 2s, and 2p orbitals, are included in the CCI calculations. The number of configurations ranged from 26 193 to 298 125, but this number was reduced to at most a few thousands by the contraction.

The integral calculations were carried out either with the system of programs ARGOS[57] or with the system of programs ASTERIX.[54]

Results and Discussion

$HMn(CO)_5$ Lowest Excited States. The calculated excitation energies to the lowest excited states of $HMn(CO)_5$ are reported in Table II. The electronic spectrum of $HMn(CO)_5$ is characterized by a high density of states between 25 000 cm^{-1} and 45 000 cm^{-1}, these states corresponding to either $d \rightarrow \sigma^*$ or $d \rightarrow d$ excitations. This is a consequence of the $d^6\sigma^2$ ground-state electronic configuration of $HMn(CO)_5$ with two low-lying vacant orbitals, one 3d orbital and one σ^* orbital. The experimental absorption spectrum of $HMn(CO)_5$[58] in the gas phase exhibits one broad band centered around 46 700 cm^{-1} with two shoulders at 34 500 cm^{-1} and 51 300 cm^{-1}. The intense band at 46 700 cm^{-1} and the shoulder at 51 300 cm^{-1} correspond probably to several allowed charge-transfer transitions ($^1A_1 \rightarrow {}^1A_1$ or $^1A_1 \rightarrow {}^1E$) resulting from $d_\pi \rightarrow \sigma^*$ and $d_\pi \rightarrow \pi^*$ excitations. The shoulder of low intensity at 34 500 cm^{-1} has been assigned[42] to the allowed $^1A_1 \rightarrow$ a ^1E ligand field transition, corresponding to a $d_\pi \rightarrow d_{x^2-y^2}$ excitation calculated at 33 580 cm^{-1}.

Because our interest centers mostly on the ligand field states $d \rightarrow \sigma^*$ and $\sigma \rightarrow \sigma^*$ excitations that are responsible for the photoreactivity of $HMn(CO)_5$, only one of the many $d \rightarrow \pi^*_{CO}$ excitations has been calculated. The excitation energies to the pair of low-lying ^3E states that play a key role in the photochemistry of $HMn(CO)_5$ and correspond respectively to $d \rightarrow d$ and $d \rightarrow \sigma^*$ excitations are calculated at 24 000 cm^{-1} and 33 000

(45) Daniel, C., unpublished.
(46) (a) Jaffe, R. L.; Hayes, D. M.; Morokuma, K. *J. Chem. Phys.* **1974**, *60*, 5108. (b) Goddard, J. D.; Yamaguchi, Y.; Schaefer, H. F., III *J. Chem. Phys.* **1981**, *75*, 3459. (c) Goddard, J. D.; Schaefer, H. F., III *J. Chem. Phys.* **1979**, *70*, 5117.
(47) This basis set is made from the (14, 9, 5) basis of Wachters[48] by adding an additional s function (exponent 0.3218), two diffuse p functions, and one diffuse d function. All the exponents were choosen according to the even-tempered criterion of Raffenetti.[49]
(48) Wachters, A. J. H. *J. Chem. Phys.* **1970**, *52*, 1033.
(49) Raffenetti, R. C.; Bardo, R. D.; Ruedenberg, K. In *Energy Structure and Reactivity*; Smith, D. W., McRae, W. B., Eds.; Wiley: New York, 1973; 164.
(50) Huzinaga, S. *Approximate Atomic Functions*: Technical Report, University of Alberta, Alberta, 1971.
(51) Huzinaga, S. *J. Chem. Phys.* **1965**, *42*, 1293.
(52) Siegbahn, P. E. M.; Almlof, J.; Heiberg, A.; Roos, B. O. *J. Chem. Phys.* **1981**, *74*, 2384.
(53) Siegbahn, P. E. M. *Int. J. Quantum Chem.* **1983**, *23*, 1869. The original program was interfaced for use in conjunction with the Asterix system of programs on the Cray-2[54] by Daniel, C., Speri, M., and Rohmer, M. M.
(54) Ernenwein, R.; Rohmer, M. M.; Bénard, M. *Comput. Phys. Commun.* **1990**, *58*, 305. Rohmer, M. M.; Demuynck, J.; Bénard, M.; Wiest, R.; Bachmann, C.; Henriet, C.; Ernenwein, R. *Comput. Phys. Commun.* **1990**, *60*, 127. Wiest, R.; Demuynck, J.; Bénard, M.; Rohmer, M. M.; Ernenwein, R. *Comput. Phys. Commun.* **1991**, *62*, 107.
(55) See, for instance: Matos, J. M. O.; Roos, B.; Malmqvist, P. A. *J. Chem. Phys.* **1987**, *86*, 1458.
(56) Marquez, A.; Daniel, C.; Fernandez Sanz, J. *J. Phys. Chem.*, in press.
(57) Pitzer, R. M. *J. Chem. Phys.* **1973**, *58*, 3111.
(58) Blackney, G. B.; Allen, W. F. *Inorg. Chem.* **1971**, *10*, 2763.

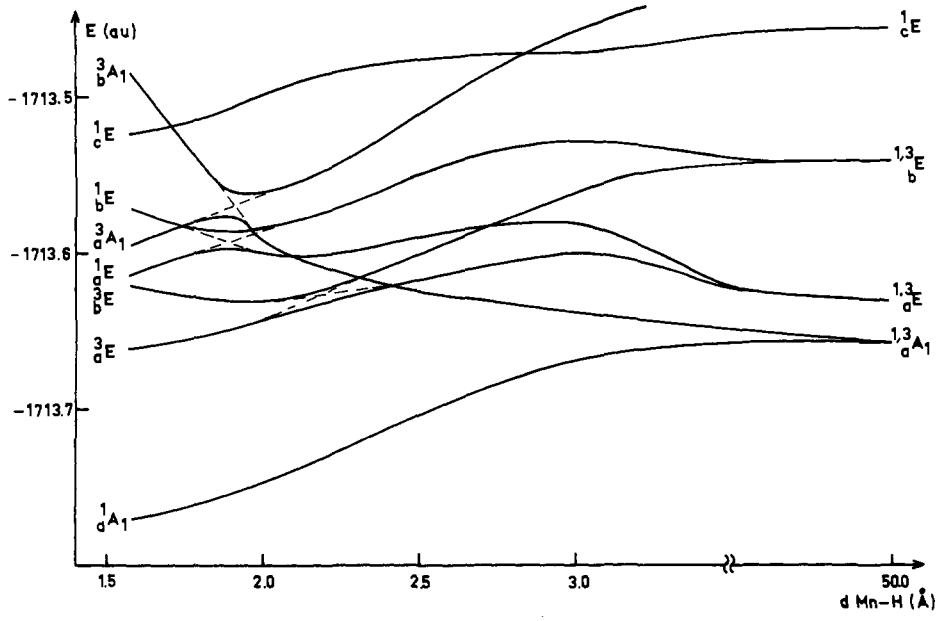

Figure 2. CCI Potential energy curves for the metal–hydrogen bond dissociation in $HMn(CO)_5$.

Table III. CCI Energy Values (in au and relative to −1713) along the Potential Energy Curves for the Reaction $HMn(CO)_5 \rightarrow H + Mn(CO)_5$ as a Function of the Distance Mn–H

	1.576 Å	2.00 Å	2.50 Å	3.00 Å	50.0 Å
b^3A_1	0.488 18	0.562 48	0.508 21	0.459 17	
c^1E	0.523 17	0.499 00	0.476 28	0.473 31	0.452 54
b^1E	0.572 57	0.585 40	0.552 82	0.530 41	0.540 89
a^3A_1	0.594 98	0.591 42	0.623 49	0.636 92	0.657 76
a^1E	0.616 19	0.600 20	0.589 83	0.584 27	0.631 24
b^3E	0.619 11	0.632 26	0.599 67	0.560 61	0.545 92
a^3E	0.660 09	0.641 94	0.617 53	0.597 52	0.632 13
a^1A_1	0.769 19	0.741 55	0.708 98	0.661 53	0.657 06

Table IV. CCI Energy Values (in au and relative to −1713) along the Potential Energy Curves for the Reaction $HMn(CO)_5 \rightarrow CO + HMn(CO)_4$ as a Function of the Distance $Mn–CO_{ax}$

	1.854 Å	2.25 Å	3.00 Å	5.00 Å	50.0 Å
b^3A_1	0.488 18	0.535 32	0.560 19	0.541 70	0.539 66
b^1E	0.572 57	0.675 42	0.581 43	0.564 42	0.561 98
a^3A_1	0.594 98	0.588 10	0.567 28	0.564 39	0.563 15
a^1E	0.616 19	0.564 42	0.667 04	0.675 42	0.674 36
b^3E	0.619 11	0.707 36	0.634 99	0.619 65	0.617 16
a^3E	0.660 09	0.619 65	0.700 22	0.707 36	0.706 05
a^1A_1	0.769 19	0.760 40	0.734 55	0.718 22	0.715 80

cm^{-1}. One important feature in this calculated electronic spectrum is the high excitation energy obtained for the b^3A_1 $\sigma \rightarrow \sigma^*$ state calculated at 61 670 cm^{-1}. This value is a consequence of the strong interaction at the equilibrium geometry between the two a^3A_1 and b^3A_1 states, the former corresponding to a 3d → 4d excitation. Two small CASSCF calculations (4e6a)[45] performed separately for the a^3A_1 state and the b^3A_1 state give an energy gap of 13 830 cm^{-1} between the two states. The highest state corresponds to the $\sigma \rightarrow \sigma^*$ excitation (77% on the corresponding configuration) with a contribution of 13% of the configuration corresponding to the 3d → 4d excitation. It is worth noting that this strong interaction between the two $^3A_1$ states will decrease with respect to the metal–hydrogen bond elongation. This is reminiscent of the tendency for certain valence levels to dissolve in the conjugate/nonconjugate Rydberg manifold observed in small systems.[59] Nevertheless, it would be hazardous to assign surely the a^3A_1 state to a Rydberg state, since the basis sets used in the calculations reported here are not adapted for describing the diffuse character of the Rydberg orbitals.[56]

Potential Energy Curves for Hydrogen Dissociation. The CCI energies for the potential energy curves corresponding to the homolysis of the metal–hydrogen bond under C_{4v} constraint are reported in Table III. The corresponding potential energy curves are shown in Figure 2. From the values of Table III, reaction 3 is calculated to be endothermic by 70.0 kcal/mol. A more accurate value of 63.0 kcal/mol is obtained when the CCI energy values are based on a CASSCF reference wave function optimized for the ground state a^1A_1.

The Mn–H bond energy in $HMn(CO)_5$ ranges from 51 to 68 kcal/mol according to the experimental data available in the literature.[60–66] From molecular orbital calculations based on functional density theory, Ziegler et al.[67] reported a value of 54 kcal/mol for the metal–hydrogen bond energy in $HMn(CO)_5$ with the error estimated to be less than 12 kcal/mol.

The $a^{1,3}E$ and $b^{1,3}E$ potential energy curves corresponding to d → d and d → σ^* excitations do not show any dissociative character with respect to the metal–hydrogen bond elongation. These two sets of PEC give rise to avoided crossings around 1.87 Å for the singlet states and 2.2 Å for the triplet states. In order to find PEC dissociative with respect to the homolysis of the metal–hydrogen bond, one has to consider the $^3A_1$ states in the vicinity of the equilibrium geometry. Namely, the a^3A_1 PEC, corresponding in its dissociative part to a σ to σ^* excitation, dissociates to the primary products H and $Mn(CO)_5$ in their ground state $a^{1,3}A_1$. The presence of an avoided crossing between the two a^3A_1 and b^3A_1 states around 1.9 Å is responsible for a small energy barrier (of the order of 10.0 kcal/mol). The PEC c^1E has been computed because the c^1E state corresponding to a d → π^* excitation is the first excited state above the avoided crossing point between the $^3A_1$ PEC susceptible of being populated through an allowed transition $^1A_1 \rightarrow {}^1E$.

Potential Energy Curves for the Loss of the Axial Carbonyl Ligand. The CCI energies for the potential energy curves cor-

(59) Robin, M. B. In *Higher Excited States of Polyatomic Molecules*; Academic Press: New York, 1985, Vol. III.

(60) Martinho Simoes, J. A.; Beauchamp, J. L. *Chem. Rev.* **1990**, *90*, 629.
(61) Connor, J. A.; Zafarani-Moattar, M. T.; Bickerton, J.; El Saied, N. I.; Suradi, S.; Carson, R.; Al Takhin, G.; Skinner, H. A. *Organometallics* **1982**, *1*, 1166.
(62) Tilset, M.; Parker, V. D. *J. Am. Chem. Soc.* **1989**, *111*, 6711.
(63) Billmers, R.; Griffith, L. L.; Stein, S. E. *J. Phys. Chem.* **1986**, *90*, 517.
(64) An upper limit of 65 kcal/mol was estimated by ref 61 from the original work of Norton et al.[65]
(65) Moore, E. J.; Sullivan, J. M.; Norton, J. R. *J. Am. Chem. Soc.* **1986**, *108*, 2257.
(66) Kristjansdottir, S. S.; Norton, J. R. In *Transition Metal Hydrides*; Dedieu, A., Ed.; VCH Publishers, Inc.: New York, 1991; pp 309–359.
(67) Ziegler, T.; Tschinke, V.; Becke, A. *J. Am. Chem. Soc.* **1987**, *109*, 1351.

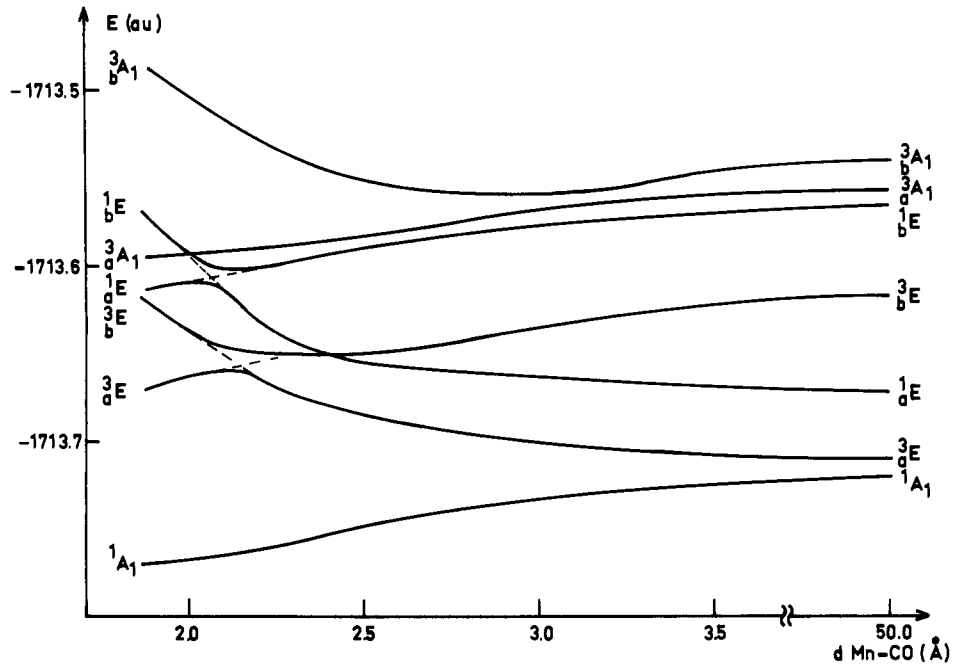

Figure 3. CCI potential energy curves for the dissociation of an axial carbonyl ligand in $HMn(CO)_5$.

Scheme III

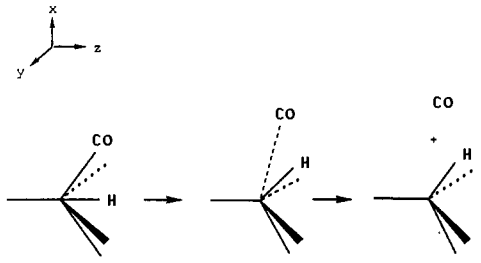

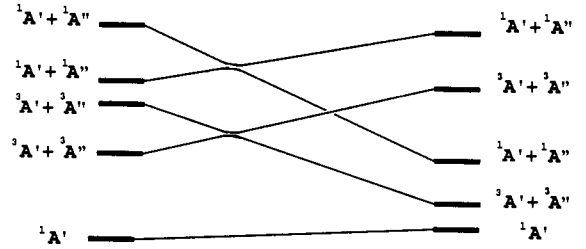

Figure 4. State correlation diagram for the dissociation of an equatorial carbonyl ligand from $HMn(CO)_5$.

responding to the loss of the carbonyl ligand under C_{4v} constraint are reported in Table IV. The corresponding potential energy curves are shown in Figure 3. From the values of Table IV, reaction 4 is calculated to be endothermic by 31 kcal/mol. A value of 30.0 kcal/mol is obtained when the CCI calculations are based on a CASSCF reference wave function optimized for the ground state a^1A_1. These values are in the range of the experimental data available for the metal carbonyl bond dissociation energy (24–42 kcal/mol) in transition metal carbonyls.[68-70] These results agree rather well with the theoretical values published on $Cr(CO)_6$, $Ni(CO)_4$, and $Fe(CO)_5$.[71,72]

The a^3A_1 state that was dissociative with respect to the metal–hydrogen bond homolysis is not dissociative with respect to the CO loss. On the contrary, the lowest $a^{1,3}E$ ligand field states are dissociative only with respect to the carbonyl loss. It is interesting to notice that the associated $a^{1,3}E$ PEC corresponds to a 3d to σ^* excitation in their dissociative part. The presence of avoided crossings between the two sets of $a^{1,3}E$ and $b^{1,3}E$ PEC gives rise to small energy barriers (less than 10.0 kcal/mol) at around 2.15 Å for the triplet state and around 2.05 Å for the singlet state. It was not necessary to compute the c^1E PEC for the reaction path corresponding to the carbonyl dissociation because two ^1E states accessible through allowed transitions ($^1A_1 \rightarrow a^1E, b^1E$) are present in the vicinity of the $a^{1,3}E$ dissociative states at the equilibrium geometry.

For the sake of simplicity we have assumed the dissociation of an axial carbonyl ligand. Since the equatorial and axial labilizations are equally probable,[41] let us now suppose that the reaction occurs through the dissociation of an equatorial ligand with the C_s symmetry retained along the reaction path (Scheme III). By this hypothesis we assume that the primary product $HMn(CO)_4$ is formed as a square pyramid with H in basal position. This is the predominant isomer identified in low-temperature matrix experiments.[28] Moreover, the relative stabilities obtained at the SCF level[45] for the two isomers of $HMn(CO)_4$ indicate that the C_{4v} structure **1** is 15.0 kcal/mol higher than the C_s structure **2**.[73]

In C_s symmetry the $a^{1,3}E$ and $b^{1,3}E$ states of $HMn(CO)_5$ are now split into two sets of $^{1,3}A' + {}^{1,3}A''$ states. The ground state of $HMn(CO)_5$ in C_s symmetry is a $^1A'$ state with two low-lying sets of $^3A' + {}^3A''$ and $^1A' + {}^1A''$ states. The corresponding state correlation diagram reported in Figure 4 exhibits the same important features as the PEC of Figure 3: (i) an allowed thermal process on the ground state $^1A'$ curve and (ii) two dissociative channels along the lowest triplet and singlet PEC with small energy barriers as a consequence of avoided crossings.

Qualitative Mechanism for the Photodissociation of $HMn(CO)_5$. From the two sets of PEC shown in Figures 2 and 3, it is possible

(68) Covey, W. D.; Brown, T. L. *Inorg. Chem.* **1973**, *12*, 2820.
(69) Bernstein, M.; Simon, J. D.; Peters, J. D. *Chem. Phys. Lett.* **1983**, *100*, 241.
(70) Lewis, K. E.; Golden, D. M.; Smith, G. P. *J. Am. Chem. Soc.* **1984**, *106*, 3906.
(71) Ziegler, T.; Tschinke, V.; Ursenbach, C. *J. Am. Chem. Soc.* **1987**, *109*, 4825.
(72) Barnes, L. A.; Bauschlicher, C. W. *J. Chem. Phys.* **1989**, *91*, 314.

(73) We have shown that the relatives stabilities of the three structures of $M(CO)_4L$ are practically unchanged when going from the SCF to the CI level.[15]
(74) Blomberg, M. R. A.; Siegbahn, P. E. M.; Nagashima, U.; Wennerberg, J. *J. Am. Chem. Soc.* **1991**, *113*, 424.
(75) Note: Since the purpose of this work is not the computation of absolute values for reaction energies and activation energies, rather limited basis sets are employed (lack of f functions on the metal, for instance). The reasonable values obtained for the endothermicities of the two processes and the small contribution given to the bonding energy by the f functions on a first-row metal (according to ref 74) justify our choice.

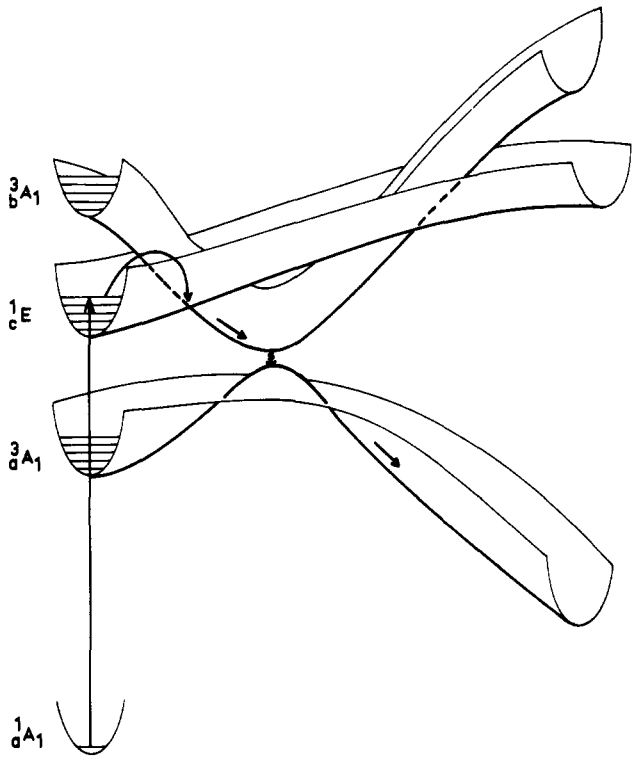

Figure 5. Mechanism proposed for the loss of hydrogen from $HMn(CO)_5$.

Scheme IV

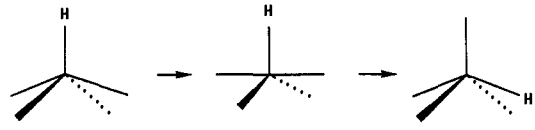

to deduce a qualitative mechanism for the hydrogen loss and the carbonyl dissociation in $HMn(CO)_5$. The proposed mechanism accounts for the occurrence of different reactive channels upon irradiation of $HMn(CO)_5$ at different wavelengths.

(i) Irradiation at the experimental wavelength of 193 nm or 51 800 cm^{-1} will bring the molecule into a vibrationally excited level of the c^1E state corresponding to a $d_\sigma \rightarrow \pi^*$ excitation (calculated at 53 990 cm^{-1} (Table II)). Intersystem crossing at a metal–hydrogen distance of about 1.70 Å will bring the system first into the b^3A_1 state and next through internal conversion into the a^3A_1 $\sigma \rightarrow \sigma^*$ state (Figure 5). From there the molecule will dissociate along the a^3A_1 PEC to the products H and $Mn(CO)_5$ in their ground state $^{1,3}A_1$.

(ii) Irradiation at the experimental wavelength of 229 nm or 43 700 cm^{-1} will bring the molecule from the ground state a^1A_1 into the b^1E state corresponding to the excitation $d_\sigma \rightarrow \sigma^*$ calculated at 43 150 cm^{-1} (Table II). From there, the molecule goes down along the b^1E PEC corresponding to the Mn–CO elongation until it reaches a potential well corresponding to an avoided crossing. At this point, the system evolves to the a^1E state through internal conversion and dissociation will then occur along the a^1E curve with the formation of the products CO and $HMn(CO)_4$ in this excited state (Figure 3). This past mechanism produces $HMn(CO)_4$ as a square pyramid with H apical **1**. The more

1 **2**

stable isomer **2** identified experimentally can be generated by a subsequent Berry pseudorotation (Scheme IV) with a mechanism similar to the one proposed for the rearrangement of $M(CO)_4L$

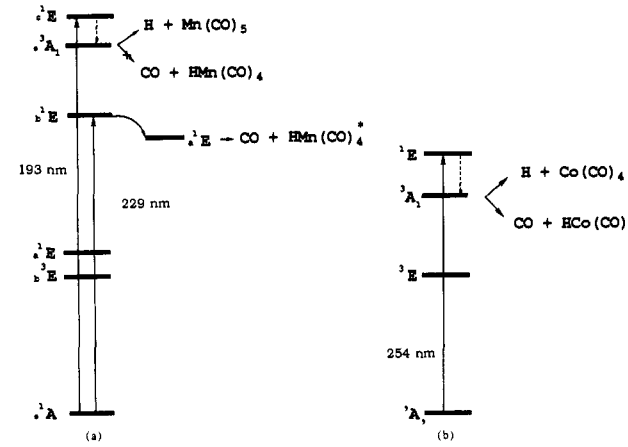

Figure 6. State diagrams for $HMn(CO)_5$ (a) and $HCo(CO)_4$ (b) (based on this work and on the results of ref 20).

fragments in the photosubstitution of d^6 metal carbonyls $M(CO)_5L$.[15] We cannot exclude a second possibility, that is, the population of the ground state a^1A_1 through an internal conversion $a^1E \rightarrow a^1A_1$ at a distance Mn–CO of 50.0 Å. From there, the recombination of $HMn(CO)_4$ and CO along the a^1A_1 PEC that regenerates $HMn(CO)_5$ in its ground state is an easy process (Figure 3).

Dissimilarity between the Photoreactivities of $HMn(CO)_5$ and $HCo(CO)_4$. Since the metal–hydrogen and metal–carbonyl bond energies are very similar for the two systems,[67,71] it is surprising that the homolysis of the metal–hydrogen bond and the carbonyl loss do occur at the same wavelength for $HCo(CO)_4$ but at different wavelengths for $HMn(CO)_5$. The principal reason for this different behavior seems to be the high density of states in the lowest part of the electronic spectrum in $HMn(CO)_5$ that is a consequence of the electronic configuration of this system. The presence of two vacant orbitals 3d and σ^* is responsible for the great number of low excited states susceptible of playing a key role in the photochemistry of $HMn(CO)_5$ compared to the situation for $HCo(CO)_4$ with only one empty orbital σ^*. Indeed, if the potential energy surfaces corresponding to the two concurrent processes are relatively simple in the case of $HCo(CO)_4$,[20] they look much more complicated (presence of avoided crossings and energy barriers) in the case of $HMn(CO)_5$. The state diagrams, not to be confounded with the state correlation diagrams, depicting the photochemistry of $HMn(CO)_5$ (Figure 6a) and $HCo(CO)_4$ (Figure 6b) outline the main differences concerning the photoreactivity of the two molecules.

The presence of a low-lying a^1E LF state in $HMn(CO)_5$ raises the energy of the b^1E state, and this is responsible for the relative high energy (calculated at 431 50 cm^{-1} in $HMn(CO)_5$ to be compared to 36 000 cm^{-1} in $HCo(CO)_4$) of the ^1E d $\rightarrow \sigma^*$ state that is photoactive for the dissociation of the carbonyl ligand. In $HCo(CO)_4$ the $^3A_1$ $\sigma \rightarrow \sigma^*$ seems to be dissociative for both the hydrogen and the carbonyl loss. The situation is quite different in $HMn(CO)_5$ where only the $^{1,3}E$ d $\rightarrow \sigma^*$ states are dissociative for the decarbonylation. In $HMn(CO)_5$, a high excitation energy will be necessary to cleave the metal–hydrogen bond because one has to reach, in the vicinity of the equilibrium geometry, a singlet state located above the potential well corresponding to the avoided crossing between the two a^3A_1 and b^1A_1 states.

Conclusion

Potential energy surfaces for the two photochemical processes of $HMn(CO)_5$ corresponding to the Mn–H bond homolysis and to the dissociation of a carbonyl ligand have been computed for the ground and excited states from CASSCF/CCI calculations. From the shape of these potential energy surfaces a mechanism has been proposed for the photochemistry of $HMn(CO)_5$ at 193 nm and 229 nm that may be summarized as follows. After excitation at 193 nm, the molecule is first excited through an allowed transition to the c^1E d $\rightarrow \pi^*$ state. From there the system may evolve first after an intersystem crossing to the b^3A_1 state

and next through an internal conversion to the a^3A_1 state. The molecule will dissociate along the a^3A_1 potential energy curve to the products H and $Mn(CO)_5$ in their ground state. Irradiation at 229 nm will bring the system into the b^1E state. From there the molecule goes down along the b^1E potential energy curve corresponding to the Mn–CO elongation until it reaches a potential well. At this point the system evolves to the a^1E state through internal conversion, and dissociation will occur along the a^1E potential energy curve with the formation of the products CO and $HMn(CO)_4$, the latter as a square pyramid with H apical.

The nature of the a^3A_1 state that raises the energy of the b^3A_1 $\sigma \rightarrow \sigma^*$ photoactive state for the metal–hydrogen bond homolysis was not clearly identified. More sophisticated calculations, with larger basis sets, similar to those reported for $Fe(CO)_5$[56] are required. It is difficult to interpret the results obtained in low-temperature matrix experiments[28] since the data are largely dependent on the experimental conditions. Gas-phase experiments would be needed in order to ascertain the mechanism of photodissociation of $HMn(CO)_5$ proposed in the present study. The main reasons responsible for the different behavior upon irradiation of $HCo(CO)_4$ and $HMn(CO_5)$ were outlined. The homolysis of the metal–hydrogen bond in monohydrides is a rather general reaction, although it may be obscured in some systems by the competition with the photoelimination of other ligands. The general ocurrence of these two photoreactions results from the dissociative character of the potential energy curves associated with a certain type of excited state. From this study and the previous one,[20] it is clear that the homolysis of the metal–hydrogen bond results from the dissociative character of the potential energy curve for the triplet state corresponding to a $\sigma_{M-H} \rightarrow \sigma^*_{M-H}$ excitation. The dissociative character of the curve associated to the $d \rightarrow \sigma^*_{M-H}$ excitation is responsible for the ligand dissociation.

Further work is needed in order to understand the photochemical behavior of other $RMn(CO)_5$ systems as a function of the fragment R. The understanding of the influence of a π acceptor ligand on the photoreactivity of these complexes through the presence of a low-lying metal-to-ligand charge-transfer state is another challenge.

Acknowledgment. The author is grateful to Dr. A. Veillard, Pr. R. L. Sweany, and Pr. M. Poliakoff for helpful discussions. The calculations have been carried out on the CRAY-2 computer of the CCVR (Palaiseau, France) through a grant of computer time from the Conseil Scientifique du Centre de Calcul Vectoriel pour la Recherche.

Registry No. $HMn(CO)_5$, 16972-33-1.

Stabilities of Hydrocarbons and Carbocations. 1. A Comparison of Augmented 6-31G, 6-311G, and Correlation Consistent Basis Sets

Janet E. Del Bene,*,† Donald H. Aue,*,‡ and Isaiah Shavitt*,§

Contribution from the Departments of Chemistry, Youngstown State University, Youngstown, Ohio 44555, University of California at Santa Barbara, Santa Barbara, California 93106, and The Ohio State University, Columbus, Ohio 43210. *Received July 1, 1991*

Abstract: Ab initio calculations have been performed at correlated levels of theory on several hydrocarbons and carbocations in order to investigate the basis set dependence of their computed hydrogenolysis energies, which determine the stabilities of these species relative to H_2 and CH_4, and from which proton affinities, hydride ion affinities, and isomerization energies may be derived. One series of basis sets studied is derived from the 6-31G(d,p) basis by augmentation with diffuse functions on carbon and additional first and second polarization functions on carbon and hydrogen. Also studied, to a more limited extent, is the triple-split 6-311G(2df,2pd) basis. The 6-31G and 6-311G series of basis sets are compared with the correlation-consistent polarized valence double-, triple-, and quadruple-ζ basis sets of Dunning, in which the sp part of the basis is systematically improved as the polarization space is augmented. The hydrogenolysis energies computed with the 6-31G basis sets show poorer convergence patterns upon augmentation, including divergence from experimental values in some cases, and show an excessive dependence on the presence of diffuse functions on carbon and on the choice of five versus six components for d polarization functions. These problems are attributed to an inadequate representation of the sp part in the valence double-split 6-31G basis sets. Better results, and reduced sensitivity with respect to the number of d components and to the addition of diffuse functions, are found with the triple-split 6-311G(2df,2pd) basis set. The correlation-consistent basis sets have been found to show smooth convergence of the computed hydrogenolysis energies, both internally and with respect to experimental data, and no significant dependence on the presence of diffuse functions or on the number of components for the d functions, except for the double-split member of the series. The correlation-consistent polarized valence triple-ζ basis set is recommended for accurate calculations of reaction energies, with 6-311+G(2df,2pd) (with diffuse functions) a reasonable alternative.

Introduction

As part of a continuing investigation of basis set and correlation effects on computed reaction energies,[1-7] we have embarked on a project to investigate reaction energetics of hydrocarbons and carbocations.[8] Our aim is to determine the level of theory which provides agreement with experimental data to within 1–3 kcal/mol, close to the uncertainty limits of many of the experiments, for computed proton affinities of hydrocarbons, hydride ion affinities of carbocations, and isomerization energies of both neutral and charged species. To accomplish this goal, it is necessary to assess the basis set, correlation, and geometry dependence of the computed properties. Such a detailed assessment is particularly important if we want to ensure that the chosen level of theory is

† Youngstown State University.
‡ University of California at Santa Barbara.
§ The Ohio State University.

(1) Del Bene, J. E. *J. Comp. Chem.* **1989**, *5*, 603.
(2) Del Bene, J. E. *Struct. Chem.* **1990**, *1*, 19.
(3) Del Bene, J. E.; Shavitt, I. *Int. J. Quantum Chem., Quantum Chem. Symp.* **1989**, *23*, 445.
(4) Del Bene, J. E.; Shavitt, I. *J. Phys. Chem.* **1990**, *94*, 5514.
(5) Del Bene, J. E.; Shavitt, I. *Int. J. Quantum Chem., Quantum Chem. Symp.* **1990**, *24*, 365.
(6) Del Bene, J. E.; Stahlberg, E. A.; Shavitt, I. *Int. J. Quantum Chem., Quantum Chem. Symp.* **1990**, *24*, 455.
(7) Del Bene, J. E.; Shavitt, I. *THEOCHEM* **1991**, *80*, 499.
(8) Del Bene, J. E.; Aue, D. H.; Shavitt, I. Part 2, to be published.

0002-7863/92/1514-1631$03.00/0